

# Soft Matter

Accepted Manuscript



This is an *Accepted Manuscript*, which has been through the Royal Society of Chemistry peer review process and has been accepted for publication.

*Accepted Manuscripts* are published online shortly after acceptance, before technical editing, formatting and proof reading. Using this free service, authors can make their results available to the community, in citable form, before we publish the edited article. We will replace this *Accepted Manuscript* with the edited and formatted *Advance Article* as soon as it is available.

You can find more information about *Accepted Manuscripts* in the [Information for Authors](#).

Please note that technical editing may introduce minor changes to the text and/or graphics, which may alter content. The journal's standard [Terms & Conditions](#) and the [Ethical guidelines](#) still apply. In no event shall the Royal Society of Chemistry be held responsible for any errors or omissions in this *Accepted Manuscript* or any consequences arising from the use of any information it contains.

## **Influence of intercalating perfluorohexane into the lipid shell on nano and microbubbles stability**

Radwa H. Abou-Saleh<sup>a,b</sup>, Sally A. Peyman<sup>a</sup>, Benjamin R. G. Johnson<sup>a</sup>, Gemma Marston<sup>c</sup>, Nicola Ingram<sup>c</sup>, Richard Bushby<sup>d</sup>, P. Louise Coletta<sup>c</sup>, Alexander F. Markham<sup>c</sup>, and Stephen D. Evans<sup>a\*</sup>

a. Molecular and Nanoscale Physics Group, School of Physics and Astronomy, University of Leeds, LS2 9JT, United Kingdom,

b. Biophysics Group, Department of Physics, Faculty of Science, Mansoura University, Egypt

c. Leeds Institute of Molecular Medicine, Wellcome Trust Brenner Building, St. James's University Hospital, Leeds, LS9 7TF, UK

d. School of Chemistry, University of Leeds, LS2 9JT, UK

**Corresponding Author:** s.d.evans@leeds.ac.uk

**Running Title:** Controlling *in vivo* MB Lifetimes

## Abstract

Microbubbles have potential diagnostic and therapeutic agents. *In vivo* stability is important with the bubbles required to survive multiple passages through heart and lungs to permit targeting, and delivery. Here we have systematically varied key parameters affecting microbubble lifetime to significantly increase *in vivo* stability. Whilst shell and core composition are found to have important role in improving microbubble stability, we show that inclusion of small quantities of C<sub>6</sub>F<sub>14</sub> in the microbubble bolus significantly improves lifetime. Our results indicate that the C<sub>6</sub>F<sub>14</sub> inserts into lipid shell, decreasing surface tension, to 19 mN/m, and increasing shell resistance, as well as saturating the surrounding medium. Surface area isotherms suggest that C<sub>6</sub>F<sub>14</sub> incorporates into the acyl chain region of the lipid, at high molar ratio indicating ~2 perfluorocarbon molecule per 5 lipid molecules. The resulting microbubble boluses exhibit higher *in vivo* image intensity, compared to the commercial compositions as well as longer lifetimes.

**Keywords:** Microbubbles, Stability, Lifetime, Microfluidics, Perfluorocarbons, Lipid shell

## 1 Introduction

Microbubbles (MBs) used for contrast enhanced ultrasound (CEUS) imaging are micron sized gas encapsulated spheres, stabilized with a shell made of biocompatible material such as proteins, surfactants, phospholipids or polymers. These MBs are capable of circulating in the vasculature and their high acoustic impedance mismatch with the surrounding tissue leads to strong ultrasound scattering resulting in enhanced contrast in US imaging. Recently there has been considerable interest in the development of MBs as vehicles for drug delivery<sup>1,2</sup> by loading them with drug-filled liposomes, or attaching genes to the shell<sup>3-5</sup>, or using a therapeutic gas in the core<sup>6,7</sup>. The MB complex can be targeted to the required location using antibodies, or other ligands, to provide a route for targeted, triggered delivery<sup>8</sup>. Further, it has been demonstrated that bursting the MBs, using an ultrasound pulse, gives rise to sonoporation of cells in the immediate vicinity of the MBs leading to enhanced therapeutic uptake<sup>9, 10</sup>. Their changing role requires that MBs be re-engineered to improve their functional performance, key MB parameters being; size and dispersity, biocompatibility, shell stiffness and MB lifetime<sup>5, 11</sup>.

For clinical and preclinical applications MBs are typically desired to be between 1-8  $\mu\text{m}$  in diameter. Control over size can be achieved by selecting a suitable production technique. Sonication and mechanical agitation are the common methods for MB production<sup>12, 13</sup>, these produce broad poly-disperse size distributions with polydispersity index of  $\sim 150\%$ , with the majority of MBs being in the range  $< 8 \mu\text{m}$ <sup>14</sup> and are currently used for diagnostic imaging<sup>15, 16</sup>. Coaxial electrohydrodynamic atomisation<sup>14, 17</sup> produces bubbles which can be of controllable size between 1 and 25  $\mu\text{m}$  and with a moderate dispersity index  $\sim 30\%$ . For highest quality monodisperse MB production the best control over size and dispersity index has come through the use of flow-focus microfluidic (MF) technology<sup>18-21</sup>. However, in this approach the MB concentration tends to be low ( $\sim 10^6$  MB/ml) compared to the  $10^8$  MB/ml used in a single bolus for *in vivo* imaging experiment. Recently Peyman *et al.* introduced a rapid pressure-drop on a chip, which led to the production of nano and micron sized bubbles typically less than 2  $\mu\text{m}$  in diameter, at high concentrations ( $>10^{10}$  and  $10^8$  MB/ml respectively)<sup>22</sup>. Post production MBs are prone to fusion and dissolution unless they are stabilized with a suitable coating. Further, such MBs should not only be stable *in vitro* but also *in vivo* where they are required to survive multiple passages through heart and lungs for

successful diagnostic imaging and possibly longer for therapeutic applications for effective targeting and release of drug payloads.

Control over the *in vitro* and *in vivo* stability (or lifetime) of MBs depends upon three main considerations; i) the conditions of the surrounding medium such as temperature, pressure and concentration of dissolved gas, ii) the MB shell composition (as a control of surface tension and the resistance to permeation) and iii) the solubility of the encapsulated gas core in the medium<sup>23</sup>. In 1950 Epstein and Plesset introduced a model describing the rate of growth and/or dissolution of “shell-less” or “uncoated” bubbles in aqueous media and showed that this is critically dependent on gas diffusion away from the bubble surface,  $D_w$ , the degree of saturation of the solution,  $f$  ( $=C_0/C_s$ ) and the initial bubble radius,  $r$ . Where  $C_0$  is the concentration of dissolved gas and  $C_s$  the concentration at saturation<sup>24</sup>. More recently Borden and Longo suggested a modified version of the Epstein-Plesset equation (1) that included the effect of the MB coating as a barrier for gas diffusion,  $R_{shell}$ , and a modifier of the surface tension,  $\sigma$ <sup>25</sup>.

$$\frac{-dr}{dt} = \frac{H}{\frac{r}{D_w} + R_{shell}} \left( \frac{1 + \frac{2\sigma}{P_0 r} - f}{1 + \frac{4\sigma}{3P_0 r}} \right) \quad (1)$$

Where  $H$ ; is the Ostwald coefficient for the gas (the ratio of the gas concentration in aqueous phase to that in the gas phase in contact with the aqueous phase)<sup>26, 27</sup>.

The Laplace pressure,  $\Delta P$ , places the gas core under increased pressure due to surface tension and curvature effects and thus provides a strong driving force for MB dissolution<sup>28</sup>. The inclusion of surfactants, in our case lipids, at the gas/liquid interface significantly reduces the surface tension and consequently the Laplace pressure<sup>29, 30</sup>. Such surfactants also provide a resistive barrier,  $R_{shell}$ , to gas leaving the MB and dissolving into the aqueous phase. Important shell properties that affects the bubble stability are surface tension, surface hardening, and resistance to gas transport<sup>30-32</sup>. Borden and Longo<sup>25</sup> showed that MB stability is strongly dependent on the lipid shell resistance and increases with increasing acyl chain length of the lipids<sup>33-36</sup>. They also showed that increasing the acyl chain length between DPPC (16) to DBPC (24) increases the lipid rigidity (Wrinkling threshold) and consequently the MB stability and circulation time. The use of higher molecular weight, less soluble, gases such as SF<sub>6</sub> and perfluorocarbons (PFCs) also significantly enhances MB lifetime and permits diagnostic and therapeutic applications<sup>5, 23, 27, 37</sup>. Several groups have investigated the effect of different gases, or gas mixtures, on the MB stability. Sarker *et al.*<sup>27, 38</sup> developed a

modified EP model for gas diffusion from MBs filled with air and PFC gas and showed that the dependence of shell permeability to gas type predicts a 500x increase in the time taken for MB dissolution for PFC compared to air filled bubbles. Kraft *et al.* used acoustical methods, to investigate the effect of the gas composition on the size and stability of shelled MBs. Using bubbles filled with nitrogen and saturated with perfluorohexane, they reported that the PFC gas increases the compressibility of the lipid monolayer resulting in more flexible and stable MBs<sup>39, 40</sup>. Kabalnov *et al.*<sup>26, 41</sup> presented a detailed model and *in vivo* experimental studies on the efficacy of different PFCs gases (as osmotic agents) mixed with oxygen or nitrogen on MB dissolution in the blood stream. They showed an increase in the bubble lifetime with increasing molecular weight of the osmotic agent, when mixed with oxygen. Increasing the PFC molecular weight beyond C<sub>6</sub>F<sub>14</sub> doesn't have a positive effect. Finally, Schutt *et al* encapsulated a mixture of different PFCs, in their gaseous state showing that MB containing mixtures of C<sub>4</sub>F<sub>10</sub> and C<sub>6</sub>F<sub>14</sub> persist for 3 min, which was longer than with either gas on its own.<sup>28, 42</sup>

The combined effect of saturation of the surrounding medium,  $f$ , and different MB shell,  $R_{\text{shell}}$ , have been investigated by Kwan and Borden in 2010<sup>43</sup>. Sulphur hexafluoride, SF<sub>6</sub> was encapsulated in SDS or lipid shell MBs and used in a modified perfusion chamber to observe the MB dissolution behaviour in SF<sub>6</sub> or air saturated medium. When suddenly placed in an air-saturated medium, MBs initially grow (air influx) and then decrease in size as a result of SF<sub>6</sub> efflux. Lipid coated MBs deviated from the model, when placed in an air saturated environment, the initial growth regime was shorter and it was followed by rapid non-uniform dissolution to the original diameter, then a steady dissolution with constant wall velocity and final stability at around 10  $\mu\text{m}$  in diameter.

For the studies reported here, MF-MBs were produced with an average diameter of 2  $\mu\text{m}$ . The stability of the population was examined *in vitro*, at 37°C, and *in vivo* using mouse models. The aim of the study was to optimize the *in vivo* lifetime of MF-MBs. Factors investigated include; shell resistance,  $R_{\text{shell}}$ , through control over lipid compositions and gas dissolution, ( $D_w$ ,  $f$ ,  $H$ ), through control over the molecular weight of gas and saturation surrounding medium. By optimising these we achieved prolonged lifetime of MBs *in-vivo*. Our optimised MBs have lifetimes >14 minutes *in vivo* and also retain excellent ultrasound contrast enhancement properties.

## 2 Materials and Methods

### 2.1 Materials:

The lipids used throughout this study were 1,2-dipalmitoyl-*sn*-glycero-3-phosphocholine (DPPC), 1,2-Distearoyl-*sn*-glycero-3-phosphocholine (DSPC), 1,2-distearoyl-*sn*-glycero-3-phosphoethanolamine-N-[methoxy (polyethylene-glycol) -2000] (DSPE-PEG<sub>2000</sub>), and 1,2-dipalmitoyl-*sn*-glycero-3-phosphoethanolamine-N-[methoxy(polyethyleneglycol)-5000 (DPPE-PEG<sub>5000</sub>) which were purchased from Avanti Polar Lipids (Alabaster, AL, USA) and used without further purification. All lipids were received in the powder form, and then dissolved in 50/50 chloroform/methanol.

### 2.2 Microbubble preparation and characterisation

The lipid composition as specified for each MB formulation was prepared as described previously<sup>19,44</sup>. Briefly, the lipid mixture was dried under a steady stream of nitrogen gas on the vial walls. This dried film was then suspended in a solution containing 4 mg/mL NaCl (where from, purity grade) and 1% glycerine (purity, Sigma-Aldrich, St. Louis, MO, USA) to a final lipid concentration 1mg/mL unless otherwise specified. This solution was vortexed for 1 minute before being placed in ultrasonic bath for 1 hour. The lipid solutions were allowed to cool down in the fridge for 5 minutes prior to use in the MF-MB maker.

Polymethylmethacrylate (PMMA) MF-chips designed in Leeds and produced by Epigem plc (Redcar, UK) were used to prepare MBs according to our previously described protocols, in which gas is flow focussed through a nozzle before being rapidly expanded to create a microspray regime<sup>19</sup>. Two gases were investigated of different molecular weight Perfluoropropane gas (C<sub>3</sub>F<sub>8</sub>), Mw=188 g/mol, and Perfluorobutane (C<sub>4</sub>F<sub>10</sub>), Mw=238 g/mol. The gas pressure was controlled using a Kukuke microprecision regulator (RS supplies, Leeds, UK). The liquid phase, containing the lipid products, was flow rate controlled using an Aladdin AL 2000 syringe pump (World Precision Instruments, Stevenage, UK). The flow rate was fixed for all MB preparations at 80µl/min. In some cases Tetradecafluorohexane (C<sub>6</sub>F<sub>14</sub>), Sigma-Aldrich, St. Louis, MO, USA, was used to saturate the lipid solution (10µl)

A typical production run produced 1 mL of MB. For each MB population formed, a 10 µl sample (collected from the middle of the homogenous MB solution) was diluted 10-fold to facilitate counting and sizing bubbles. From this diluted sample 30 µl was introduced in a 50

$\mu\text{m}$  chamber on a glass slide. The MBs were allowed to rise for  $\sim 1$  minute before acquiring images. An inverted microscope (Nikon, Japan) was used to image the MBs on a 60x magnification. A CCD camera (DS-Fil 5Mega pixel, Nikon, Japan) was used to capture 40 images for each sample, from which the concentration and size distribution were obtained using *Image J* freeware (<http://rsbweb.nih.gov/ij/>) and statistically analysed using Origin Pro (Version 8.5 or later).

### 2.3 *In vitro* Lifetime

MB lifetime was measured *in vitro* as described previously<sup>45</sup>. Briefly, 500 $\mu\text{l}$  MB solution was introduced in 500  $\mu\text{l}$  cell medium [RPMI from Invitrogen, Life Technologies, UK with 10% (v/v) foetal calf serum (Sigma Aldrich, UK)] and incubated at 37  $^{\circ}\text{C}$  in a digital dryblock heater (Model D1100, Labnet International, USA). The vial containing the sample was left open exposed to air and 10  $\mu\text{l}$  samples were collected every 15 min for sizing and counting.

### 2.4 *In vivo* Lifetime

For *in vivo* measurements 50 to 100 $\mu\text{l}$  MB solutions (in PBS) were injected via a syringe attached to a tail vein catheter. The injection of the MB bolus was controlled by a syringe driver at a rate of 0.6mL/min. A typical bolus contained  $\sim 10^8$  MBs in 100  $\mu\text{l}$ .

All animal work was performed under licence and in accordance with the UK Animals (Scientific Procedures) Act 1986 following local ethical review and procedures. Eighteen athymic CD1-nu/nu male mice (6–8 weeks old) were maintained in individual ventilated cages under specific pathogen-free conditions with free access to diet and water.

The mouse aorta was identified and imaged by pulsed wave (PW) Doppler imaging using a Vevo770 (FUJIFILM VisualSonics, Inc.) using the 40 MHz transducer. For post-processing analysis, a region of interest (ROI) was drawn within the aorta such that the ROI was maintained within the aorta for the whole video loop, ensuring that with respiration motion, the ROI was not sampling tissue outside the aorta as indicated by the blue circle in Figure 2A. In Figure 2B, shows a snapshot showing the accumulation of the MBs in the aorta post injection.



## 2.5 Langmuir Trough:

A Langmuir trough (KSV Nima) was used to measure the differences in monolayer compressability and elasticity. The trough was equipped with two movable PTFE barriers to compress the monolayer symmetrically. A Wilhelmy plate tensiometer (paper method) was used to measure the surface pressure of the monolayer. This experiment was performed for the same lipid monolayer composition found to form the most stable MBs. 20ul of a 1mg/mL solution of (DPPC+5% DSPE-PEG2000), in chloroform, was spread on the surface of a subphase of water in presence and absence of C<sub>6</sub>F<sub>14</sub>. Pressure-Area isotherms were made with the barriers compression rate set to 5 mm/min and the surface pressure was not allowed to rise beyond 30 mN/m, this ensured reversability of the isotherms and allowed us to observe multiple compression /expansion cycles which is important for determination of whether material is lost from the monolayer during compression.

## 3 Results

### 3.1 Microbubble Production and Characterisation:

MBs were prepared in the spray regime of a specially designed MF-chip<sup>19</sup> shown schematically in Figure 3A. The image (inset) in Figure 3B shows a typical MB population, with an average MB diameter of 1.7±1.1 µm and concentrations ~2x10<sup>9</sup> MB/mL. No bubbles were produced with a diameter > 7 µm.

### 3.2 MB lifetime:

*In vitro* MBs lifetime was initially determined by measuring the MB concentration, using optical microscopy, every 30 min in a closed vial at room temperature and atmospheric pressure. MB concentration versus time (*in vitro* results) for MBs prepared with shells of DPPC (or DSPC) with 10% DSPE-PEG<sub>2000</sub> encapsulating C<sub>3</sub>F<sub>8</sub> gas was tested (see **Supp.1**). The data showed that the MBs were relatively long lived in both cases, i.e. for both lipid types, with no significant difference in their stability over a period of ~3 hr following production. In contrast, the *in vivo* lifetime, as determined from time-intensity curves (TICs) in the mouse aorta, showed that both MBs decayed within 2 minutes *in vivo*. A slightly higher acoustic intensity signal was observed for the DPPC MBs compared to the DSPC ones, this is consistent with previous observations for such MBs.<sup>46</sup> These initial results showed that the *in vitro* study of MBs, at room temperature and atmospheric pressure, are not good indicators of

the *in vivo* behaviour and that physiological conditions (increased temperature, pressure and potential for gas exchange) around the MBs are likely to significantly affect the MB stability. Thus, in order to better test our MBs under more realistic conditions the *in-vitro* experiment was modified to using cell medium (RPMI with 10% (v/v) foetal calf serum) incubated at 37 °C and leaving the sample in an open tube exposed to air for gaseous exchange. Based on the *in vivo* data (**Supp.1**), and that DPPC MBs have more homogenous lipid distribution on the bubble shell<sup>47</sup>. The slightly shorter DPPC (16:0) lipid was chosen for subsequent MB studies over the DSPC (18:0). A series of factors were investigated to detect their effect on MB stability, firstly *in vitro* and then *in vivo*. These included; i) the degree of pegylation in the MB shell, which affects the potential for phase separation<sup>45,48</sup>, ii) the gas core by switching to a heavier gas (C<sub>4</sub>F<sub>10</sub>) to reduce solubility and diffusivity in the surrounding medium and finally iii) factors related to the surrounding solution, such as super saturating the lipid solution with C<sub>3</sub>F<sub>8</sub> gas prior to bubble production, also increasing the concentration of NaCl in the lipid solution to over 0.1M to prevent bubble fusion<sup>49</sup>.

Of the factors identified above only two showed a significant effect on MB stability. Summary data, taken from a larger data set of the variables investigated is detailed in the supplementary section (**Supp2**). The first significant effect was that on changing from the C<sub>3</sub>F<sub>8</sub> core to the high molecular weight C<sub>4</sub>F<sub>10</sub> gas, the MB population displayed a doubling in lifetime from the order of one to two hours (at 37 °C) Figure 4A. This effect is well understood and is due to a reduced solubility of the higher MW gas in solution (Ostwald coefficient reduces from  $5.2 \times 10^{-4}$  for C<sub>3</sub>F<sub>8</sub> to  $2.0 \times 10^{-4}$  for C<sub>4</sub>F<sub>10</sub>) and a slightly reduced diffusion rate in water (from  $7.45 \times 10^{-10}$  for C<sub>3</sub>F<sub>8</sub> to  $6.9 \times 10^{-10}$  for C<sub>4</sub>F<sub>10</sub>) and an increase in the resistance of the shell to the increased MW. These effects have been modelled in (**Supp3**) following the work of Sarkar *et al.*<sup>27,38</sup> for MBs with different cores and assuming the surface tension of the shelled MB to be 25 mN/m.

Decreasing the PEG concentration from 10% to 5% led to a modest increase in the average lifetime (**supp4**). However, in spite of this significant improvement in *in vitro* lifetime, at body temperature, these formulations showed negligible improvement in the *in vivo* MB lifetime, as indicated in the TIC curves (**supp4**).

To control the saturation, *f*, or solubility of the gas in the solution, *H*, the medium containing the MBs was saturated with C<sub>6</sub>F<sub>14</sub>, a liquid at room temperature. The solubility of C<sub>6</sub>F<sub>14</sub> in water, at 25 °C, is  $2.7 \times 10^{-4}$  mol/L which is equivalent to  $\sim 0.05$   $\mu$ L for 1mL of lipid solution<sup>11</sup>,

<sup>50</sup>. The volume of  $C_6F_{14}$  per mL of MB was varied between 0 and 15  $\mu\text{L}/\text{mL}$  of the lipid solution (DPPC+5%DSPE-PEG<sub>2000</sub>) to determine the optimum concentration at which the MBs have the longest lifetime. Figure 4B shows the fraction of bubbles remaining, in medium at 37 °C, as a function of time for different volumes of  $C_6F_{14}$  added to a 1 mL MB bolus. The data shows that MB lifetime was significantly increased upon the addition of  $C_6F_{14}$  for concentrations  $\geq 6\mu\text{L}/\text{mL}$  with the 15 $\mu\text{L}/\text{mL}$  sample producing the most stable MB population. However, the addition of such volumes of  $C_6F_{14}$  adversely affected the MB production leading to a 10-fold reduction in the concentration of MBs produced. Thus the addition of 10  $\mu\text{L}$   $C_6F_{14}$  was selected as being optimal. At this concentration MBs were still produced a high concentration  $\sim 1 \times 10^9$  MB/mL whilst also increasing MBs stability. The MB decay rate was reduced to only 0.07 % over the 2 hr period.

Figure 4C shows the calculated MB population profile expected based on the calculation that a typical MB distribution, given in Figure 3B, and that the MBs decay in accordance with the modified Epstein Plesset model proposed by Borden<sup>25</sup> and Sarkar<sup>27</sup>. In these models the surface tension was assumed to be 25 mN/m and the saturation,  $f$ , was taken as unity, and all other parameters are given in the supplementary material. We note that in this model MBs of diameter  $< 0.5 \mu\text{m}$  were considered to be not observable optically and so bubbles are removed from the MB population when their size decreases below 0.5  $\mu\text{m}$ . Essentially we see the expected trend that  $C_4F_{10} > C_3F_8$  however we note that the model predicts longer lifetimes than experimentally observed probably indicating that the MB surface tension, shell resistance and/or the degree of saturation are not accurately modelled in our system.

Figure 5A show the *in vivo* TIC for four different MB variants, comparing both the effect of the presence of  $C_6F_{14}$  in the bolus and the concentration of the lipid. Comparison of the area under the curves for the cases with and without  $C_6F_{14}$  clearly indicates that the presence of  $C_6F_{14}$  significantly enhances MB persistence in the bloodstream. Further, by doubling the lipid concentration, from 1 mg/mL to 2 mg/mL, during the production of the MBs, the concentration of MB was doubled from  $1 \times 10^9$  to  $2 \times 10^9$  MB/mL and lifetime was modestly enhanced leading to a larger area beneath the TIC. Figure 5B shows the TIC curves for our best *in vivo* MB in comparison to those obtained using commercially available MBs (Micromarker (MM), Definity).

For each MB population the intensity versus time curves were collected from 5 mice, from each curve 6 different parameters were extracted, Figure 6A, that can facilitate the

comparison of the different MBs and aid the determination of the one with the best properties for *in vivo* imaging. These parameters are presented with the codes as: 1- Rate of decay. This can be calculated from the slope of the curve after the peak point. The smaller the decay rate the longer the MB lifetime. 2- Peak enhancement, which is the point at the highest contrast intensity, this mainly depends on the MB shell properties and concentration. 3- Area under curve, which is proportional to both the MB concentration and persistence time. A greater area indicates better quality and stability of MBs. 4- Time to peak, which is the time to reach the maximum intensity at the ROI. It is better if this is short. 5- Peak enhancement duration, which is the point of time with the highest contrast intensity after injection. 6- Time to half peak contrast. The longer this parameter is, the more prolonged the lifetime is of the MBs at the ROI.

Figure 6B shows the data analysis for the TIC curves comparing the six parameters between our in-house MF-MBs and the commercially available MBs. The data suggests that the MF-MBs produced in-house, display improved peak enhancement and area under curve, and the significantly longer time to half peak.

In order to understand the role of  $C_6F_{14}$  in enhancing MB lifetime, a Langmuir trough was used to plot the relation between surface pressure,  $\Pi$  (mN/m) versus average molecular area, for a 1mg/mL (DPPC+5%PEG<sub>2000</sub>) solution spread at the air/water interface in the presence and absence of  $C_6F_{14}$  in the sub-phase. Figure 7 shows compression isotherms of the monolayer. All conditions are fixed for both cases with the only difference being the sub-phase, either just with milliQ water or MilliQ water plus  $C_6F_{14}$  at the same concentration used during MB production (10  $\mu$ l/mL).

The mean molecular area was found to increase from 0.5 nm<sup>2</sup> to 0.63 nm<sup>2</sup> upon the inclusion of  $C_6F_{14}$  in the sub-phase, which indicates the incorporation of the  $C_6F_{14}$  molecules within the lipid layer. The fractional component of  $C_6F_{14}$  in the MB shell was calculated to be 0.4, which means an estimation of 2 PFC molecules for every 5 lipid molecules. As a consequence of incorporating  $C_6F_{14}$  (surface tension 11 mN/m<sup>51</sup>) with this proportion in the lipid layer, the surface tension of the monolayer is reduced from 25 mN/m<sup>27,38</sup> to 19 mN/m. Consequently, this leads to a reduction in the Laplace pressure from 50x10<sup>3</sup> N/m -in absence of  $C_6F_{14}$ - to 38x10<sup>3</sup> N/m, in presence of  $C_6F_{14}$ , which leads to improved estimate in the MB lifetime. The hollow circles, Figure 4c, indicate the predicted enhancement in MB lifetime due to the reduction in surface tension. This is shown more clearly in **supp3**.

The isothermal compressibility,  $C$ , and the compression modulus (elasticity),  $K$ , are calculated from the extrapolated lines shown on the isotherm, of the lipid modified interface. These calculations showed that the existence of PFC in the surrounding solution increased the compressibility ( $C$ ) from  $1.0 \times 10^{-2}$  to  $1.2 \times 10^{-2}$  m/mN, which is corresponding to a decrease in elasticity ( $k$ ) from 97 mN/m to 88 mN/m in presence of PFC molecules. These results are in good agreement with the previously published work by Krafft<sup>39</sup> on the effect of saturating the surrounding air with different PFC gases on the compressibility and elasticity of lipid monolayers.

#### 4 Discussion and conclusion:

MB lifetime stability has been investigated by changing different factors that are known to have an effect on MB lifetime. The MB architectures have a shell comprising of a DPPC/DSPE-PEG<sub>2000</sub> binary system the components of which are completely miscible below 15% PEG<sub>2000</sub> concentrations forming a single condensed phase with low permeability<sup>52</sup>. We have previously shown that reducing the PEG<sub>2000</sub> concentration from 10 to 5% helped increase the MB lifetime<sup>45</sup>. MB lifetime was also improved by changing the encapsulated gas from C<sub>3</sub>F<sub>8</sub> to one with a larger molecular weight, C<sub>4</sub>F<sub>10</sub>. This decreases the coefficient of diffusivity from  $7.45 \times 10^{-10}$  to  $6.9 \times 10^{-10}$  m<sup>2</sup>/sec<sup>27</sup>. Combining the changes outlined above has resulted in a considerable improvement in *in vitro* MBs lifetimes, as discussed in the results section above.

Recently, C<sub>6</sub>F<sub>14</sub> has been encapsulated together with Dox, or gold nano-rods in nanoparticles and locally activated at the site of tumour to form MBs, C<sub>6</sub>F<sub>14</sub> had shown to enhance acoustic imaging, cavitation and therapeutic delivery effect<sup>53, 54</sup>. In this work; saturating the medium surrounding the MBs with liquid C<sub>6</sub>F<sub>14</sub> and using C<sub>4</sub>F<sub>10</sub> in the gas core is considered a key improvement in the MB lifetime. The presence of C<sub>6</sub>F<sub>14</sub> in the surrounding medium increased the stability and lifetime of MBs *in vitro* and showed an improvement up to 14 mins *in vivo* Figure 5. We believe this improvement in stability arises for two reasons (Figure 8); firstly, the C<sub>6</sub>F<sub>14</sub> effectively results in the saturation of the surrounding medium, reducing the ability for C<sub>4</sub>F<sub>10</sub> to partition in to the aqueous phase. Secondly, the incorporation of C<sub>6</sub>F<sub>14</sub> molecules into the lipid shell of the MB as concluded from Figure 7 leads to a 25% reduction in the surface tension of the membrane, and hence the Laplace driving force for dissolution. This also modifies the mechanical properties of the shell, where a 17 % increase in the compressibility is observed accompanied with a 10% decrease in the shell elasticity. The

effect of saturating the gas medium with PFC gases on lipid monolayers has been studied by Gerber et al.<sup>55, 56</sup>, who saturated the atmosphere above Langmuir monolayer of DPPC with vapours of C<sub>6</sub>F<sub>14</sub>. They reported that saturating the gaseous medium with PFC gas has a fluidizing effect on DPPC monolayers adsorption at the gas/water interface, as it prevents the liquid condensed phase formation and hinders lipid crystallisation. Krafft et al.<sup>39</sup> also demonstrated that DMPC lipid shell MBs, showed a 20% increase in compressibility of the membrane and 26% decrease in the surface tension upon saturating air with C<sub>6</sub>F<sub>14</sub> in the gas medium. Krafft and Fainerman et al.<sup>57, 58</sup> theoretically modelled and practically showed that in case of DPPC monolayers saturating the gas phase with C<sub>6</sub>F<sub>14</sub> led to C<sub>6</sub>F<sub>14</sub> molecules being adsorbed at the lipid surface and causing a reduction in the energy of attraction between the DPPC molecules, which leads to a fluidization of the monolayer. From the data shown here it appears that the surface tension alone is not a significant enough change to account for the increased MB stability and thus we also believe that the inclusion of the C<sub>6</sub>F<sub>14</sub> molecules into the lipid chain must also increase the shell resistance.

*In vivo* MB lifetime improved from 2 min to 14 min through a combination of changes to the lipid shell, the gas core and the addition of C<sub>6</sub>F<sub>14</sub> to medium. Further, comparing in-house MF-MBs and commercial MBs (Figure 5) showed that the sat-C<sub>6</sub>F<sub>14</sub> MBs provided enhanced lifetime and contrast properties compared to their commercial counterparts.

In conclusion, controlling MBs properties i.e decay rate, intensity and enhancement duration, was achieved by changing the phospholipid shell composition, the encapsulated gas and most significantly the saturation of the surrounding medium with C<sub>6</sub>F<sub>14</sub>. Our data suggests the C<sub>6</sub>F<sub>14</sub> molecules are incorporated in the lipid shell reducing the surface tension and also increasing the mechanical compressibility and collapse pressure. MBs for drug delivery applications are likely to require longer lifetimes to allow for accumulation at the ROI for optimal dose delivery and will thus benefit greatly from such improvements.

## 5 Acknowledgments:

Authors would like to acknowledge EPSRC for funding (EP/I000623, EP/K023845) and thank the Microbubble Consortium (<http://www.microbubbles.leeds.ac.uk/>) at the University of Leeds for useful discussions.

The data presented in this article are openly available from the University of Leeds Data Repository <http://doi.org/10.5518/68>

## 6 References

1. S. B. Feinstein, *Am J Physiol Heart Circ Physiol*, 2004, **287**, H450-457.
2. J. R. Lindner, *Nature Reviews*, 2004, **3**, 527-532.
3. B. Geers, I. Lentacker, N. N. Sanders, J. Demeester, S. Meairs and S. C. De Smedt, *Journal of control Release*, 2011, **152**, 249-256.
4. J. R. McLaughlan, N. Ingram, R. H. Abou-Saleh, S. Harput, T. Evans, S. D. Evans, L. Coletta and S. Freear, Prague, 2013.
5. E. C. Unger, T. Porter, W. Culp, R. LaBell, T. Matsunaga and R. Zutshi, *Adv Drug Deliver Rev*, 2004, **56**, 1291-1314.
6. J. Zhang, Y. Luan, Z. Lyu, L. Wang, L. Xu, K. Yuan, F. Pan, M. Lai, Z. Liu and W. Chen, *Nanoscale*, 2015, **7**, 14881-14888.
7. F. Cavalieri, I. Finelli, M. Tortora, P. Mozetic, E. Chiessi, F. Polizio, T. B. Brismar and G. Paradossi, *Chemical materials*, 2008, **20**, 3254-3258.
8. B. Geers, I. Lentacker, N. N. Sanders, J. Demeester, S. Meairs and S. C. De Smedt, *J Control Release*, 2011, **152**, 249-256.
9. R. Chen, Y. Luan, Z. Liu, W. Song, L. Wu, M. Li, J. Yang, X. Liu, T. Wang, J. Liu and Z. Ye, *BioMed research international*, 2015, **2015**, 514234.
10. Y. Luan, Z. Chen, G. Xie, J. Chen, A. Lu, C. Li, H. Fu, Z. Ma and J. Wang, *Journal of nanoscience and nanotechnology*, 2015, **15**, 1357-1361.
11. E. G. Schutt, D. H. Klein, R. M. Mattrey and J. G. Riess, *Angew Chem Int Ed Engl*, 2003, **42**, 3218-3235.
12. C. Christiansen, H. Kryvi, P. C. Sontum and T. Skotland, *Biotechnology and applied biochemistry*, 1994, **19 ( Pt 3)**, 307-320.
13. G. Pu, M. A. Borden and M. L. Longo, *Langmuir*, 2006, **22**, 2993-2999.
14. E. Stride and M. Edirisinghe, *Med Biol Eng Comput*, 2009, **47**, 883-892.
15. J. R. Lindner, M. P. Coggins, S. Kaul, A. L. Klibanov, G. H. Brandenburger and K. Ley, *Circulation*, 2000, **101**, 668-675.



16. J. R. Lindner, P. A. Dayton, M. P. Coggins, K. Ley, J. Song, K. Ferrara and S. Kaul, *Circulation*, 2000, **102**, 531-538.
17. U. Farook, H. B. Zhang, M. J. Edirisinghe, E. Stride and N. Saffari, *Med Eng Phys*, 2007, **29**, 749-754.
18. M. Hashimoto and G. M. Whitesides, *Small*, 2010, **6**, 1051-1059.
19. S. A. Peyman, R. H. Abou-Saleh, J. R. McLaughlan, N. Ingram, B. R. G. Johnson, K. Critchley, S. Freear, J. A. Evans, A. F. Markham, P. L. Coletta and S. D. Evans, *Lab on a chip*, 2012, **12**, 4544-4552.
20. E. Talu, K. Hettiarachchi, R. L. Powell, A. P. Lee, P. A. Dayton and M. L. Longo, *Langmuir*, 2008, **24**, 1745-1749.
21. E. Talu, K. Hettiarachchi, S. Zhao, R. L. Powell, A. P. Lee, M. L. Longo and P. A. Dayton, *Mol Imaging*, 2007, **6**, 384-392.
22. S. A. Peyman, J. R. McLaughlan, R. H. Abou-Saleh, G. Marston, B. R. Johnson, S. Freear, P. L. Coletta, A. F. Markham and S. D. Evans, *Lab Chip*, 2016, **16**, 679-687.
23. J. J. Kwan and M. A. Borden, *Adv Colloid Interfac*, 2012, **183**, 82-99.
24. P. S. Epstein and M. S. Plesset, *Adv Colloid Interfac*, 1950, **183**, 82-99.
25. M. A. Borden and M. L. Longo, *Langmuir*, 2002, **18**, 9225-9233.
26. A. Kabalnov, D. Klein, T. Pelura, E. Schutt and J. Weers, *Ultrasound Med Biol*, 1998, **24**, 739-749.
27. K. Sarkar, A. Katiyar and P. Jain, *Ultrasound Med Biol*, 2009, **35**, 1385-1396.
28. *United states Pat.*, US 6,953,569 B2, 2005.
29. H. D. Van Liew and M. E. Burkard, *Advances in experimental medicine and biology*, 1997, **411**, 395-401.
30. D. E. Yount, *Aviation, space, and environmental medicine*, 1979, **50**, 44-50.
31. H. D. Van Liew and S. Raychaudhuri, *Journal of applied physiology*, 1997, **82**, 2045-2053.
32. C. Li, J. Chen, J. Wang, Z. Ma, P. Han, Y. Luan and A. Lu, *The Science of the total environment*, 2015, **521-522**, 101-107.



33. B. A. Lewis and D. M. Engelman, *J Mol Biol*, 1983, **166**, 211-217.
34. K. H. Kim, S. Q. Choi, J. A. Zasadzinski and T. M. Squires, *Soft Matter*, 2011, **7**, 7782-7789.
35. D. H. Kim, M. J. Costello, P. B. Duncan and D. Needham, *Langmuir*, 2003, **19**, 8455-8466.
36. J. J. Kwan and M. A. Borden, *Soft Matter*, 2012, **8**, 4756-4766.
37. K. Ferrara, R. Pollard and M. Borden, *Annu Rev Biomed Eng*, 2007, **9**, 415-447.
38. A. Katiyar and K. Sarkar, *J Colloid Interface Sci*, 2010, **343**, 42-47.
39. C. Szijjarto, S. Rossi, G. Waton and M. P. Krafft, *Langmuir*, 2012, **28**, 1182-1189.
40. S. Rossi, G. Waton and M. P. Krafft, *Langmuir*, 2010, **26**, 1649-1655.
41. A. Kabalnov, J. Bradley, S. Flaim, D. Klein, T. Pelura, B. Peters, S. Otto, J. Reynolds, E. Schutt and J. Weers, *Ultrasound Med Biol*, 1998, **24**, 751-760.
42. *United States Pat.*, 5,605,673, 1997.
43. J. J. Kwan and M. A. Borden, *Langmuir*, 2010, **26**, 6542-6548.
44. R. H. Abou-Saleh, S. A. Peyman, K. Critchley, S. D. Evans and N. H. Thomson, *Langmuir*, 2013, **29**, 4096-4103.
45. R. H. Abou-Saleh, S. D. Evans and N. H. Thomson, *Langmuir*, 2014, **30**, 5557-5563.
46. T. V. Rooij, Y. Luan, G. Renaud, A. F. W. van der Steen, M. Versluis, N. De Jong and K. Kooiman, *Ultrasound in medicine and biology*, 2015, **41**, 1432-1445.
47. K. Kooiman, T. J. A. Kokhuis, T. V. Rooij, I. Skachkov, A. Nigg, J. G. Bosch, A. F. W. van der Steen, W. A. van Cappellen and N. De Jong, *European Journal of lipid science and technology*, 2014, **116**, 1217-1227.
48. A. K. Kenworthy, S. A. Simon and T. J. McIntosh, *Biophysical Journal*, 1995, **68**, 1903-1920.
49. B. W. Ninham and P. Lo Nostro, in *Molecular forces and self assembly: in colloid, nano science and biology*, Cambridge university press, USA, 2010, ch. 8, pp. 232-249.
50. A. S. Kabalnov, K. N. Makarov and O. V. Scherbakova, *Journal of fluorine chemistry*, 1990, **50**, 271-284.

51. Y. Luan, J. Xu, B. Huang, X. Liu, Y. Liu, L. Chen and X. Chu, *Zhonghua xue ye xue za zhi = Zhonghua xueyexue zazhi*, 2015, **36**, 286-290.
52. M. M. Lozano and M. L. Longo, *Soft Matter*, 2009, **5**, 1822-1834.
53. J. Zhong, S. Yang, L. Wen and D. Xing, *J Control Release*, 2016, **226**, 77-87.
54. N. Zhang, X. Cai, W. Gao, R. Wang, C. Xu, Y. Yao, L. Hao, D. Sheng, H. Chen, Z. Wang and Y. Zheng, *Theranostics*, 2016, **6**, 404-417.
55. F. Gerber, M. P. Krafft, T. F. Vandamme, M. Goldmann and P. Fontaine, *Angew Chem Int Ed* 2005, **44**, 2749-2752.
56. F. Gerber, M. P. Krafft, T. F. Vandamme, M. Goldmann and P. Fontaine, *Biophysical journal*, 2006, **90**, 3184-3192.
57. M. P. Krafft, V. B. Fainerman and R. Miller, *Colloid Polym Sci* 2015, **293**, 3091-3097.
58. V. B. Fainerman, E. V. Aksenenko and R. Miller, *Adv Colloid Interface Sci*, 2015, DOI: 10.1016/j.cis.2015.11.004.

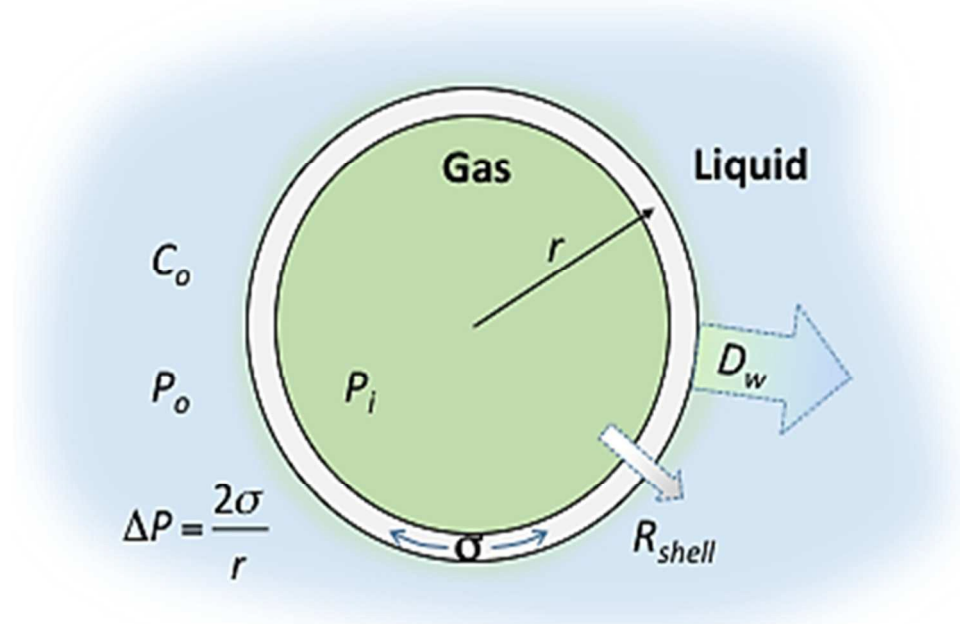


Figure 1: Schematic representation of a lipid shelled MB illustrating the factors that affect MB lifetime. The different terms are defined in the text.

254x190mm (96 x 96 DPI)

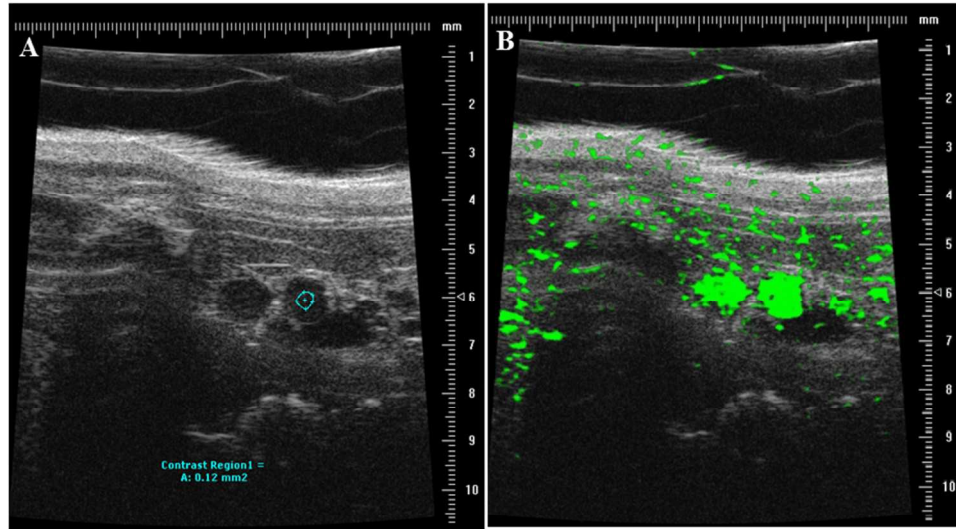


Figure 2: In vivo imaging of mouse aorta with high frequency ultrasound. (A) A region of interest (ROI) within the aorta was selected for post processing analysis (blue region) to determine the contrast intensity within the aorta over time. (B) example image showing the aorta post injection filled with MBs.

254x190mm (96 x 96 DPI)

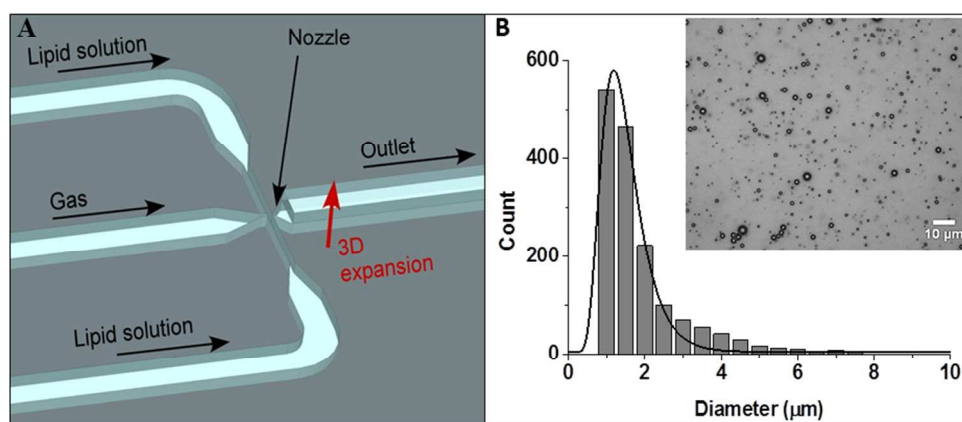


Figure 3: Bubble production and characterisation. (A) A schematic of the microfluidic chip design emphasizing the 3D expansion region for the production of MBs in the spray regime. (B) Graph displaying the size distribution for one of the bubble populations. The inset shows a bright field image representing the produced MBs (sample is 10-fold diluted).

254x190mm (96 x 96 DPI)

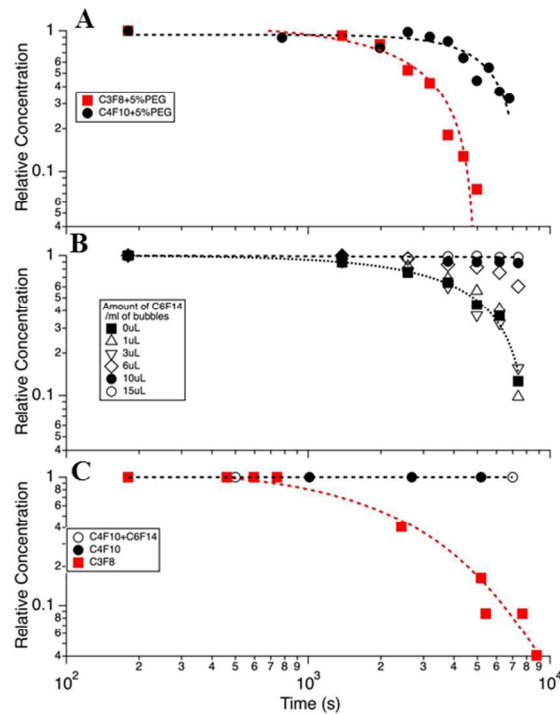


Figure 4: (A) shows the MB concentration versus time for DPPC + 5% PEG DSPE MBs with C3F8 and C4F10 gas cores. (B) the effect of adding liquid C6F14 to the MB bolus, in increasing amounts from 0 to 15  $\mu$ L/mL, has on influencing MB lifetime. (C) calculated lifetime expected for the MB distribution profile shown in Fig. 3 for 3 cases, i) with a C3F8 core, ii) with a C4F10 core and iii) C4F10+ C6F14 (open circles). The parameters for calculations were taken from Sarkar26 and given in detail in (supp4). All data taken at 37  $^{\circ}$ C in cell media and at atmospheric pressure.

254x190mm (96 x 96 DPI)

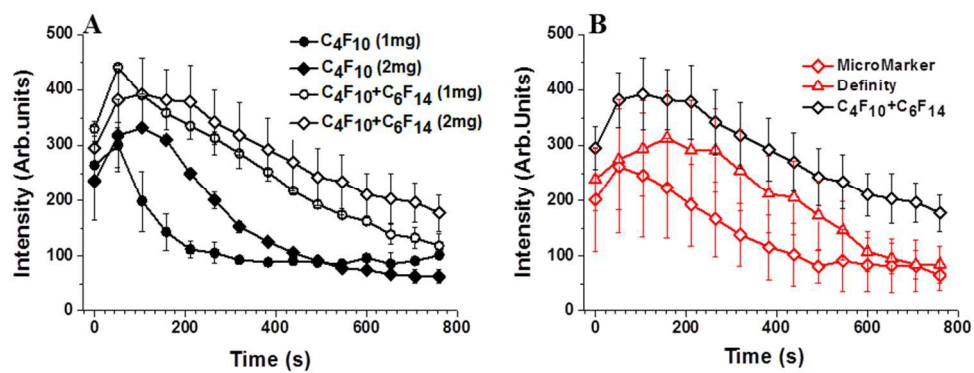


Figure 5: Ultrasound time intensity curves in mice Aorta. (A): Shows the effect of increasing the final lipid concentration, and saturating the lipid solution with C6F14 on MBs lifetime for MBs made with DPPC+5%PEG2000 and encapsulating C4F10 gas. (B): Compares TIC curves for our improved in-house MBs and commercial MBs.

254x190mm (96 x 96 DPI)

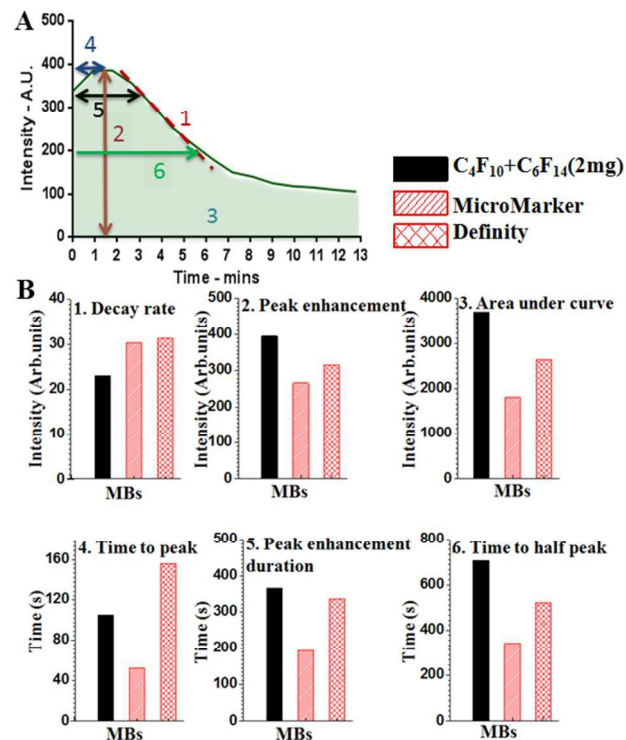


Figure 6: In vivo TIC analysis. (A) Shows an example Time Intensity Curve (TIC) for MB flow in a mouse aorta and defines six key parameters for defining MB lifetime, 1) is the decay rate calculated from the slope of the curve after the peak intensity, the slower decay rate the greater the MB stability, 2) Peak enhancement, is the maximum intensity signal, this is due to the MB shell properties as well as the gas used, 3) Area under the curve, indicates the signal from the total MB population present and therefore the concentration of MBs, 4) Time to peak, this is the time to reach the peak signal intensity, it should be short enough to enable imaging within a realistic time-frame, 5) Peak enhancement duration, is the length of time the MB signal persists, this needs to be of sufficient duration to allow a useful imaging session following MB injection 6) Time to half peak, the time it takes the signal to reduce half the peak intensity which is a further measure of the duration of signal. (B) The six parameters for our in-house MBs and two commercial MB formulations. In-house MBs showed (1) slower decay rate, (2) improved peak enhancement signal and duration (5), (3) larger area under curve, (4) shorter time after injection to reach the maximum intensity, (6) and significantly longer time to half peak, indicating better in vivo stability, better contrast enhancement and longer imaging time.

254x190mm (96 x 96 DPI)



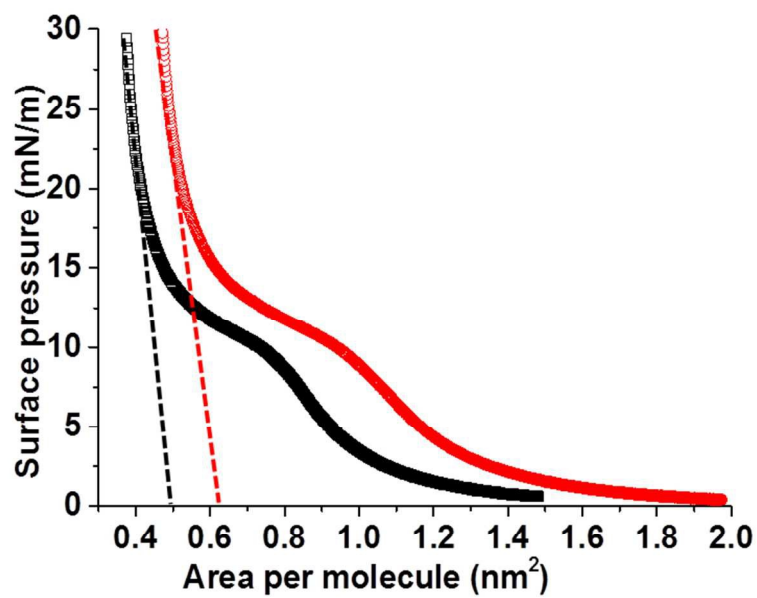


Figure 7: Langmuir isotherms of DPPC+5% DSPE-PEG2000 monolayers, on water sub-phase (black) and water with 10  $\mu\text{L/mL}$  C6F14 added to the sub-phase (red). Dashed lines show extrapolated average molecular area for DPPC/DSPE-PEG2000 phase

254x190mm (96 x 96 DPI)

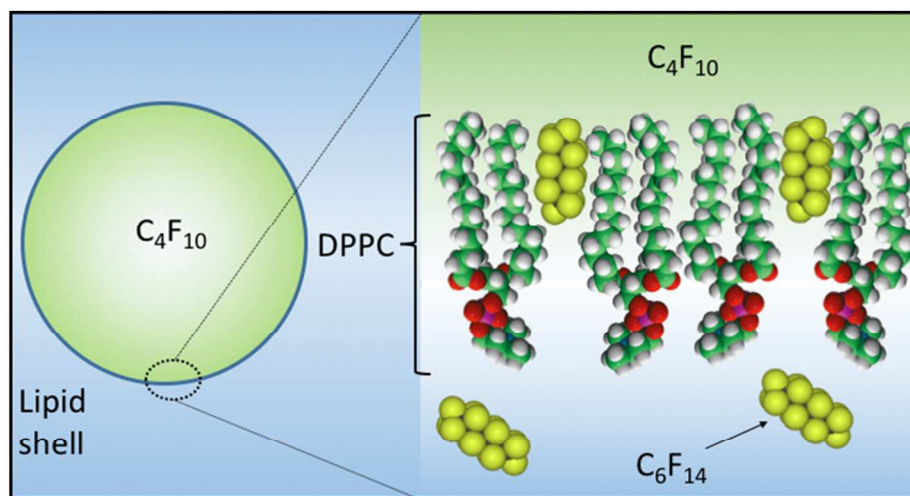
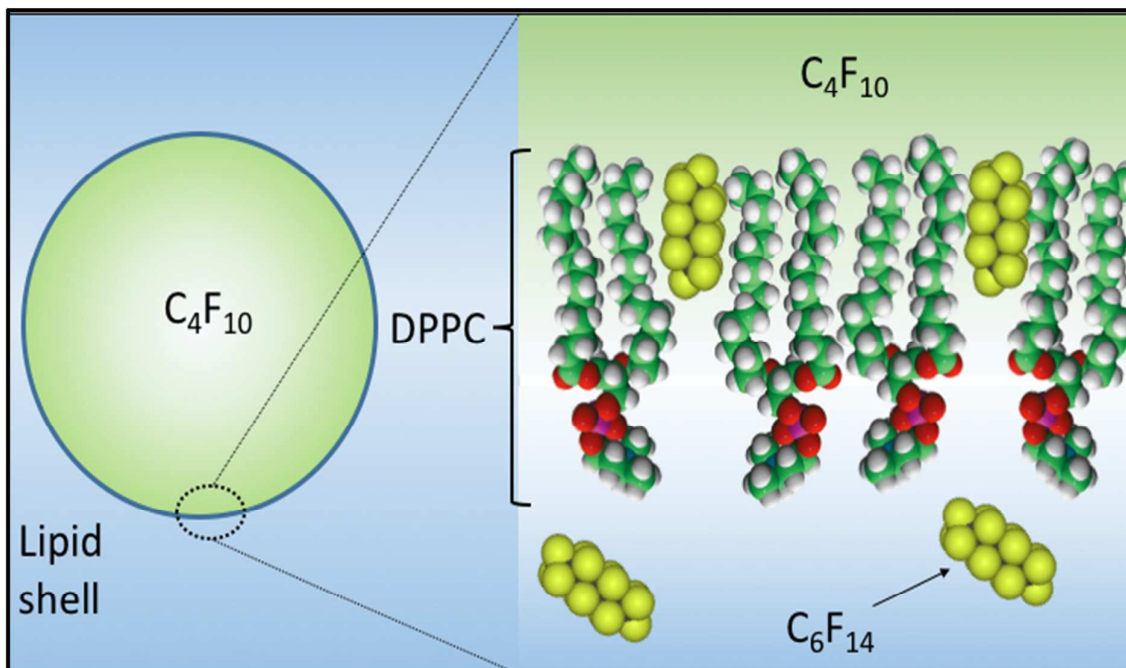


Figure 8: Schematic diagram showing i) the incorporation of  $C_6F_{14}$  into the MB shell thereby reducing surface tension and the Laplace driving force for dissolution and ii) the saturation of the medium with  $C_6F_{14}$  thereby reduces the solubility of  $C_4F_{10}$  in ambient phase.

254x190mm (96 x 96 DPI)



Incorporating  $C_6F_{14}$  in the lipid shell enhances microbubbles *in vivo* lifetime by reducing surface tension. It saturates the medium and reduces diffusivity of  $C_4F_{10}$ .